Internal Lipid Content and Viscoelastic Behavior of Wool Fibers

M. Marti,[1] A. M. Manich,[1] M. H. Ussman,[2] I. Bondia,[1] J. L. Parra,[1] L. Coderch[1]

[1]*IIQAB (CSIC), Jordi Girona 18-26, 08034 Barcelona, Spain*
[2]*Universidade da Beira Interior (UBI), Marqués d'Avila e Bolama, 6200 Covilhâ, Portugal*

Received 26 December 2002; accepted 7 January 2004

ABSTRACT: Wool is a natural keratin fiber made up of cuticle and cortical cells held together by the cell membrane complex (CMC), which contains few internal lipids (IWLs) (1.5% by mass). IWL arouse considerable cosmetic and dermatological interest because of its high proportion of ceramides. In this work, IWLs were extracted with acetone, methanol, and dichloromethane/acetone solvents, and the possible alteration of the extracted fibers with respect to their textile feasibility was analyzed. Parameters of yield, fibril, and matrix viscoelastic behavior, deformation work, and breaking elongation were useful in highlighting the effect of internal wool lipids on the mechanical properties of the fibers. The extraction with acetone and methanol solvents supplied good yields of IWL. Although extraction with methanol achieved the richest extracts, the fibers were chemically modified. By contrast, although acetone-extracted fibers had similar properties after treatment, alkaline solubility was lower and fiber length and barb were superior. In the mechanical analysis, a prior extraction of IWL increased yield tenacity and decreased the elongation at break of the fibers, maintaining the feasibility of extracted wool for textile purposes. © 2004 Wiley Periodicals, Inc. J Appl Polym Sci 92: 3252–3259, 2004

Key words: mechanical properties; viscoelastic properties; stress; strain

INTRODUCTION

It is well known that wool fiber is made up of cuticle and cortical cells held together by the cell membrane complex (CMC), which forms the only continuous phase in keratin fiber. The complex morphological structure of fine wool fibers is shown schematically in Figure 1.

The cuticle cells, which account for approx. 10% of the fiber, constitute the outermost surface of the wool fiber, and are responsible for properties such as wettability, tactility, and felting behavior.[1]

The cortex is made up of approx. 90% of keratin fibers, and is largely responsible for their mechanical behavior. It consists of closely packed overlapping cortical cells arranged parallel to the fiber axis. Cortical cells are approximately 100 μm long and 3–6 μm wide, and they are composed of rod-like elements of crystalline proteins (microfibrils) surrounded by a relatively amorphous matrix. The low-sulphur material, with a simple regular structure and without crosslinks, forms crystalline fibrils, which are embedded in a matrix of more complicated and crosslinked high-sulphur material. The fibrillar protein forms first, and the low-sulphur parts of the natural block copolymer crystallize in parallel rods separated by the high-sulphur domains. Then the rest of the high sulphur protein is formed and solidifies the matrix. Nature joins the two constituents of this natural composite in a special way. The low-sulphur protein molecules in the fibrils have high-sulphur domains that come out of the fibrils at intervals and are crosslinked to the rest of the amorphous matrix.[2]

As stated above, the cuticle and cortical cells are separated by a continuous network, the cell membrane complex. This accounts for approx. 3.5% of the fiber, is around 25 nm in width, and provides adhesion between the cells. The CMC has three major components: (1) an easily swollen "intercellular cement" (1.5%) of a crosslinked nonkeratinous protein (δ-layer); (2) a lipid component (1%), which may be associated with β-layers; and (3) a chemical resistant proteinaceous membrane (1%), which surrounds each cortical and cuticle cell.

Mercer[3] stated that the physical strength of a cellular tissue is the strength of the complex of the component cells and their adhesive connections; as in a chain, this structure is no stronger than its weakest link. The β-layers, which are generally believed to arise from the hydrophobic ends of a lipid bilayer, were shown by Rogers[4] to constitute regions of relative weakness in the fiber because of splitting along these planes during the preparation of the fiber cross-sections.

Correspondence to: M. Marti (mmgesl@iiqab.csic.es).
Contact grant sponsor: the CICYT Program; contract grant number: PETRI 95-0490-OP.

Journal of Applied Polymer Science, Vol. 92, 3252–3259 (2004)

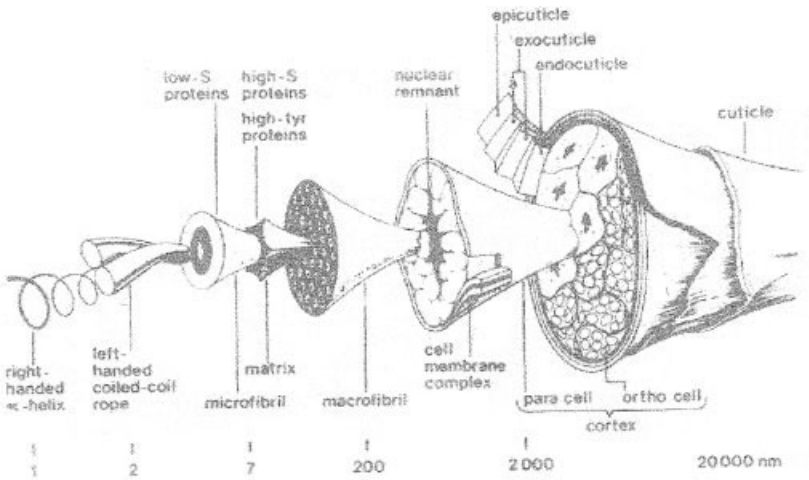

Figure 1 Schematic diagram of the morphological components of a wool fiber.

When fibers are mechanically deformed, the distortions at the macroscopic level lead to changes at the molecular level. The bonds and interactions between components of the macromolecules forming the fiber become stressed. In small strains, where the fiber acts mechanically as a linear viscoelastic material, the model of the polymer is an extension of a standard linear solid[5] with a distribution of relaxation times. Speakman[6] and many other authors refer to this as the "Hookean region" in the case of wool fiber. This designation is rather controversial given that this region is far from spring like in behavior; in fact, it resembles a mechanical behavior, approximating linear viscoelasticity as shown by Bendit,[7] who coined the term "preyield region."

When a critical stress is reached, the α-form fibril in one zone opens into the longer β-form in which the molecules are fully extended. The fibrils will double in length, and provide the high extensibility of wool. This transfers stress to the matrix alongside the fibril; the tension on the fibril drops, and the fraction that can be transformed is limited. The opening up then starts in another zone. This continues until the fibrils in all zones have been partially transformed from the α- to the β-form. Elongation increases rapidly without a notable increase in stress. This part of the curve is called the "yield region."

Increased extension stretches the matrix more, and causes the increase in stress in the postyield region in which load and extension are again proportional. Fiber breakage occurs mainly in this region.

Depending on the strain, the fiber behaves successively like a crystallized solid in the preyield region, and like an amorphous solid or a liquid in the yield region, where the fiber is said to have a plastic like response, and again like a solid in a postyield region.[8]

The preyield region shows the fiber to be homogeneously resistant to stretching. Under these circumstances, all the strain is taken up in distorting the bonding network of the fibril polymer structure. Given that the intermediate and long-range forces within the fiber represent the weaker interactions, most of the distortion present in any polymeric system arises from these weaker bonds. The yield zone represents the macromolecular chains unfolding without offering any resistance, and the postyield region shows the new fiber configuration resistant to stretching caused by matrix polymer reordering up to failure point in the case of wool.

Cosmetic and dermatological interest in IWL rich in ceramide compounds prompted us to optimize different extraction methodologies with supercritical fluids and a number of organic solvents. Evaluation of chemical and mechanical wool modifications after lipid extraction is important to determine the feasibility of this extracted wool for textile purposes. The influence of the IWL on its breaking tenacity measured in bundle form was found to be irrelevant.[9] This study seeks to clarify the role of the IWL in the viscoelastic behavior of the fiber by modeling the stress–strain curves. The viscoelastic behavior of different fiber and yarns has been used as a tool for the microstructural characterization of fiber and yarns.[10,11]

Yield parameters, fibril, and matrix viscoelastic behavior, deformation work and breaking elongation could play a role in highlighting the effect of the IWL on the mechanical properties of the fiber.

EXPERIMENTAL

Materials and methods

Raw Spanish Merino wool samples supplied by SAIPEL (Terrassa, Spain) were used for extraction, lipid analysis, and evaluation of chemical and mechanical characteristics. Wool was industrially cleaned

TABLE I
Lipid Extraction Process, Reference, and Linear Density of Tops

Lipid extraction process	Reference	Top linear density
Nonextracted wool	NEW	22.83 ktex
Methanol-extracted	METH	23.51 ktex
Acetone-extracted	ACET	31.00 ktex
Dichloromethane/acetone extracted	DCMA	25.65 ktex

in a process with five scouring becks for total degreasing. The cleaning sequence consisted of a washing at $T = 40–42°C$ (first beck), followed by a treatment with sodium carbonate at $T = 45–55°C$ (second beck), sodium carbonate, and ethoxylated nonylphenol (3rd beck), ethoxylated nonylphenol at $T = 50–52°C$ (fourth beck), and a final rinsing with water at $T = 45–47°C$ (fifth beck). Finally, the wool was heat dried.

Five kilograms of wool were extracted at pilot plant level. The extraction procedure, which consisted of a pumped-forced reflow system, was performed for 4 h with a solvent ratio of 1/40 in three organic solvents, that is, acetone, methanol, and dichloromethane/acetone (2 : 1). The extraction temperature was $T = 47–49°C$ for acetone extraction, and $T = 55–57°C$ for methanol extraction. In these two cases the temperature was lower than the boiling point of the solvents. In the third case, dichloromethane/acetone the extraction temperature was at boiling point. A kinetic control of extraction processes was also carried out, taking different aliquots at 1, 2, 3, and 4 h to be analyzed. After distillation, lipid extracts were concentrated and stored in 1 l of chloroform/methanol (2/1, v/v) at $T = -20°C$. Aliquots were dried and weighed, and lipid extraction percentages were determined.

Mechanical and chemical wool modifications after the extraction process were determined by the evaluation of a number of parameters such as fiber diameter, fiber length and barb of raw wool, and whiteness and yellowness indexes, fiber tenacity, and elongation of top wool.

Table I summarizes the processing characteristics of the wool tops supplied.

The diameter and length of the extracted wool fibers were evaluated using the Air Flow method and an Almeter Al-100, respectively, following the corresponding guidelines.[12,13] Mean diameter in μm was obtained with 2.5 g of fibers in triplicate by the Air Flow method at constant pressure. Fiber length and barb in mm were obtained by the Almeter Al-100 with 0.5 to 2.5 g of samples corresponding to 20,000 to 120,000 fibers, approximately.

Whiteness index (Berger 59) and yellowness index (ASTM D1925) of extracted tops were measured by using a spectrophotometer Color-Eye 3000 (Macbeth, USA) with D65 illuminant and a 10° observer.

In fiber stress–strain tests, fibers randomly were taken from the tops previously conditioned for 48 h in a standard atmosphere. Fiber fineness was determined by optical microscope and the stress–strain experiment was performed, using a computer programmable dynamometer (Instron 5500R) in accordance with the ASTM Standard D 3822 (1980) with some modifications. Specimen effective length was 30 mm, the deformation rate was 1%/s, and sample size was 50 fibers per top. The calculations were corrected for any slack or pretensioning in the specimen at the start of the tensile test. The initial linear region of the curve was calculated by the intersection of the straight line passing through the points at 0.4 and 0.2 of the maximum load with the displacement axis. Fibers, which break at very low strain due to weak points, were discarded. The mean breaking tenacity and elongation were obtained.

Modeling the stress–strain curves

Average stress–strain curves were calculated using the software supplied by Instron. As for the viscoelastic modelling, the "strain" X of the fibers was dimensionless (mm/mm), and the deformation gradient r was 1%/s. During the stress–strain tests, the mean tenacity of the 50 fibers F(cN/dtex) induced by strain at 0.5, 1, 1.5, 2, 2.5, 3, 3.5, 4, 5, 6, 8%, etc., up to breaking point in steps of 2% of strain were recorded for viscoelastic modeling.

The model used for fitting the stress–strain curves is a derivation of the standard linear solid element that accounts for the contribution of the two components separately: the fibrils and the matrix.[14] The behavior of the fibrils is explained by a nonlinear Maxwell element of viscosity η and by a non-inear spring of modulus M, which includes the shape exponent D,[15] affecting the deformation X, which expresses the nonlinear behavior of fibrils. The behavior of the matrix is explained by a nonlinear spring of modulus C, which includes the shape exponent E,[15] affecting the deformation X, which expresses the nonlinear behavior of the matrix. The shape exponents D and E envisage that at low strains the fibrils and the matrix are oriented into the direction of stretch. Both the fibrils and the matrix are initially considered to be slack, and that during straining they become taut and contribute to the increase in stress.[16] In Figure 2, the parameters of the mechanistic model explain the contribution of fibril and matrix components to the fiber stress during the tensile test. Both elements in parallel constitute the standard nonlinear solid element model[14] used for describing the tensile behavior of wool fibers at the r deformation rate. In the preyield region, the stiffness of the macromolecular structure is indicated by the

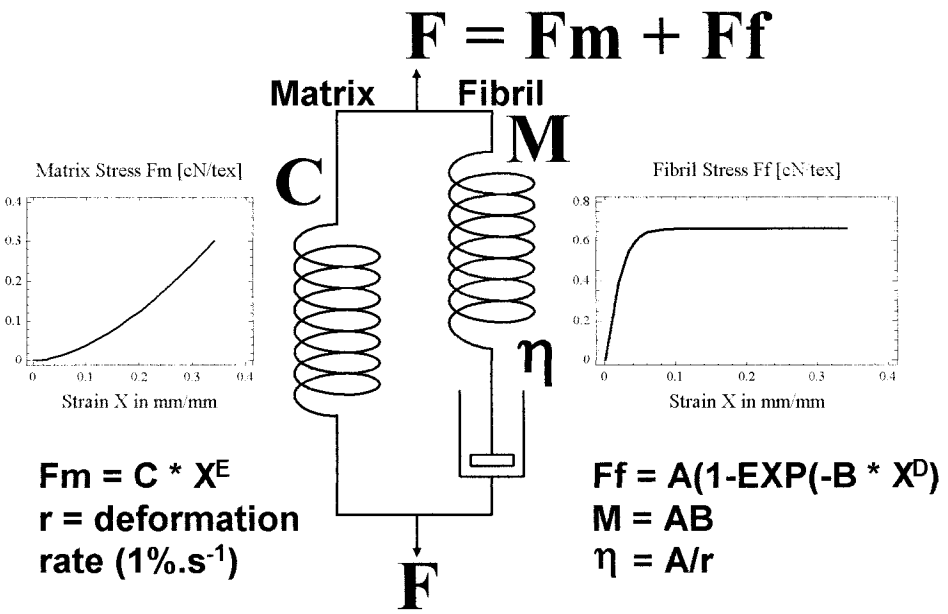

Figure 2 Standard nonlinear solid element used for describing the tensile behavior of wool fibers at deformation rate *r*. Fiber stress F is separately attributed to Ff Fibril stress and Fm Matrix stress. The model is made up of a Maxwell element with a spring of *M* modulus and a dashpot of η viscosity in parallel with a spring of *C* modulus. The nonlinearity of the model is described by the power terms *D* and *E* affecting the fibril and the matrix behavior.

initial modulus $M = AB$. The yield region begins above *A*, which represents the tenacity at which fibrils are transformed from the α- to the β-form. The speed at which the transformation is produced by strain is directly related to *B*, which is the inverse of the relaxation time $\tau = \eta/M$ of the Maxwell element. The stiffness of the postyield region is directly related to *C*.

Nonlinear regression procedures were used for model fitting. Initial estimators of the equation parameters are essential for obtaining the correct fit.[17] The initial estimators of both *D* and *E* shape exponents were unity, and the values of the initial slope *M*, the yield stress *A*, and the reinforcing modulus *C* were derived graphically from the plot. The detailed procedure of graphical estimation of the coefficients are described elsewhere.[14]

RESULTS AND DISCUSSION

Raw Spanish Merino wool was extracted at the pilot plant level to obtain lipid extract rich in ceramide compounds. It was used because its internal lipid composition resembles that found in the stratum corneum from skin.[18,19]

The extraction was performed with three solvents—acetone, methanol, and dichloromethane/acetone—extracted under conditions detailed in the experimental part (Table II).

IWL are believed to account for approx. 1.2% oww[20] to 1.5% oww.[21] Accordingly, appropriate yields were obtained with the extraction conditions used (0.7% for dichloromethane/acetone, 0.8% for acetone extraction, and 1.39% for methanol). The highest extraction value obtained with methanol should be taken into account. This has also happened with Soxhlet extraction at the laboratory level.[18]

The raw wool was carded to obtain the top wool to evaluate its properties (Table III) and tensile behavior.

According to the results, nonsignificant differences were observed in the fiber diameter value. However, the fiber length and barb values showed a marked increase in those fibers extracted with acetone (ACET), whereas only slight decreases were observed in the other two extractions. The evaluation of the whiteness and yellowness indexes of the extracted tops was carried out to confirm the possible alteration of the fibers (Table II).

Significant differences were observed in the whiteness and yellowness indexes, depending on the solvent used for the extraction. The best value of the whiteness index was obtained in acetone-extracted

TABLE II
Extraction Yield of Spanish Merino Wool (% on Wool Weight, oww)

Reference	Yield (% oww)	Whiteness Berger 59	Yellowness ASTM D1925
1. NEW	—	9.466	14.134
2. METH	1.392	6.634	19.188
3. ACET	0.820	8.282	17.459
4. DCMA	0.730	7.635	17.006

TABLE III
Determination of Physical Test Parameters on Top Wool

	Fiber diameter (μm)	Fiber length (mm)	% CV	Barb (mm)	% <25 mm	% <40 mm
1. NEW	22.9	51.6	51.7	65.3	17.7	40.4
2. METH	23.7	50.2	54.4	65.1	19.3	44.8
3. ACET	23.3	54.1	51.5	68.4	14.6	39.6
4. DCMA	23.9	51.3	49.9	64.1	15.2	40.0

fibers. This value resembled those of the nonextracted fibers. By contrast, the fibers extracted with methanol had a lower whiteness index and a higher yellowness index. This leads to a possible alteration of the fibers during the methanol extraction.

Tensile tests results

The results of tenacity and elongation at break are shown in Table IV. The values of mean tenacity induced at different strain levels are given in Table V. After the first fiber breakage, no mean tenacity values were calculated to avoid bias in the mean tenacity of the remaining fibers. The stress–strain curve was directed from that point towards the final mean tenacity and elongation at break shown in Table IV. Points are plotted in Figure 3.

Tenacity and elongation at break

Individual values of tenacity and elongation at break were examined using the Analysis of Variance technique,[22] with the result that nonsignificant differences were observed between extracted and nonextracted wool. This finding agrees with the result obtained in an earlier work,[9] where nonsignificant differences were observed in fiber tenacity of wool subjected to different extraction lipid procedures measured in bundle form. Nevertheless, significant differences were observed between the tenacity at break of the three extracted wool samples. The values of individual fiber mean tenacity with the 95% of confidence intervals are shown in Figure 4. Regarding the individual fiber elongation at break, the extraction procedures significantly decreased this parameter, although nonsignificant differences were observed between the nonextracted wool NEW and the wool extracted with methanol METH. The mean values of fiber elongation at break with the 95% confidence intervals are shown in Figure 4.

TABLE IV
Individual Fiber Mean Tenacity (cN/dtex) and Elongation (%) at Break According to the Different Lipid Extraction Procedures

Reference	Tenacity (cN/dtex)	Elongation (%)
1. NEW — Nonextracted wool	1.00 (5.3%)	34.1 (3.7%)
2. METH — Methanol-extracted	1.10 (4.6%)	33.4 (3.7%)
3. ACET — Acetone-extracted	0.92 (6.1%)	29.7 (4.5%)
4. DCMA — Dichloromethane/ acetone extracted	1.09 (4.9%)	30.8 (4.1%)

Coefficient of Variation in parentheses.

TABLE V
Values of Mean Tenacity Induced at Different Levels

Straining (mm/mm)	NEW (cN/dtex)	METH (cN/dtex)	ACET (cN/dtex)	DCMA (cN/dtex)
0.005	0.13	0.1	0.12	0.12
0.01	0.21	0.2	0.21	0.23
0.015	0.3	0.29	0.31	0.35
0.02	0.39	0.39	0.4	0.45
0.025	0.47	0.47	0.48	0.55
0.03	0.53	0.54	0.54	0.63
0.035	0.58	0.6	0.59	0.69
0.04	0.61	0.64	0.61	0.72
0.05	0.66	0.69	0.64	0.76
0.06	0.69	0.71	0.66	0.78
0.08	0.71	0.75	0.68	0.81
0.1	0.74	0.77	0.69	0.83
0.12	0.76	0.8	0.71	0.85
0.14	0.77	0.82	0.74	0.87
0.16	0.79	0.85	0.76	0.89
0.18	0.81	0.86	0.77	0.92
0.2	0.83	0.89	[a]	0.93
0.22	0.85	[a]		0.96
0.24	[a]			[a]

[a] First fiber breaking point.

Modeling the stress–strain curve

Fiber tenacity F (cN/dtex) is related to elongation X (mm of straining/mm gauge length) according to the model shown in Figure 2 as follows:

$$F = A(1 - \exp(-BX^D) + CX^E \quad (1)$$

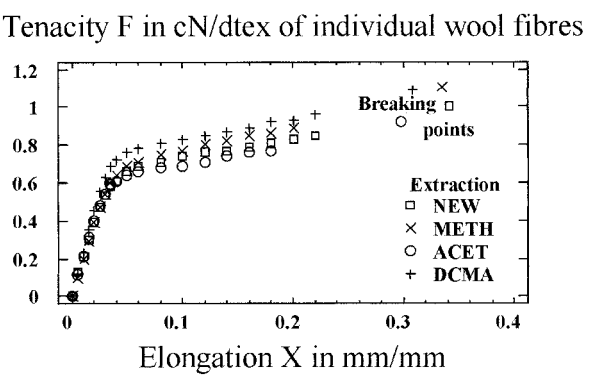

Figure 3 Experimental points of Table IV and V for plotting the mean stress–strain curve of the individual wool fiber tensile test according to the extraction method.

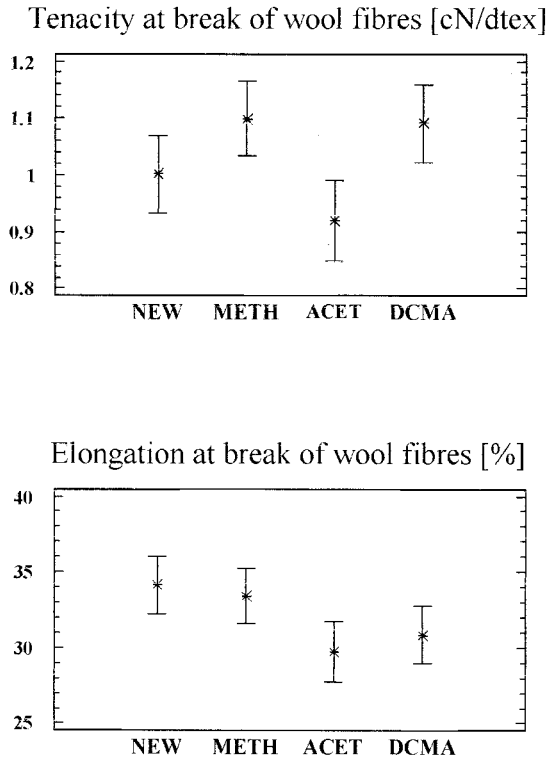

Figure 4 Tenacity at break (up) and elongation at break (down) of the individual wool fibers subjected to different lipid extraction procedures including the 95% confidence intervals.

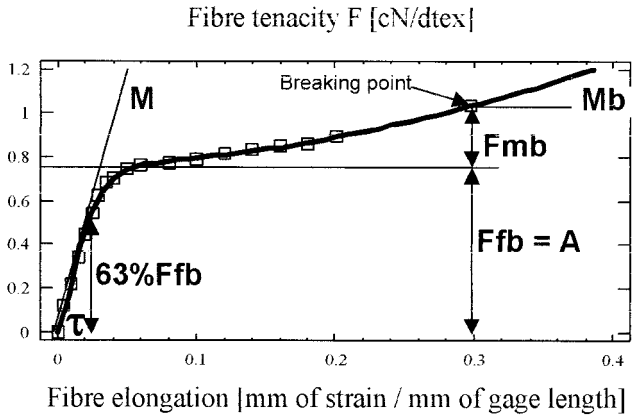

Figure 5 Individual wool fiber tenacity–elongation fitted curve. Initial modulus M. Relaxation time τ at which 63% of the yield tenacity Ffb is reached. Reinforcing modulus at break Mb and matrix tenacity at break Fmb.

Relationship between mechanistic model parameters and equation coefficients are shown in Figure 2. Equation coefficients were based on the initial estimators that are graphically derived. The initial estimators of the shape exponents D and E were regarded as unity. The initial estimators of A, B, and C were obtained from Figure 3, taking into account the relationship between yield tenacity and A, the initial modulus $M = AB$ and the reinforcing modulus C. The final estimators of the model were obtained by the application of the iterative nonlinear regression procedure.[22]

To obtain the best fit, different possibilities for the shape exponents D and E were explored. They were regarded as unity, were varied with the restriction $D = E$, or were independent. This means that the number of parameters to be estimated for the equation were 3, 4, or 5. The criterion used for the selection of the best model was to maximize the so-called adjusted R^2 according to the criterion of Draper and Smith.[17] The adjusted-R^2 coefficient is the determination coefficient R^2 of the model balanced by the degrees of freedom of the fitting $1 - (1 - R^2) \times [(n - 1)/(n - p)]$, n being the number of experimental points used for model fitting, and p, the number of the parameters of the model. Results of fitting including the determination coefficient R^2 and the adjusted-R^2 coefficient are shown in Table VI.

Discussion on viscoelastic behavior

Based on the equation parameters, we can derive the parameters of the mechanistic model, which accounts for the tensile behavior of the fiber. These are shown in Figure 5 and Table VII. The initial modulus M is related to the initial fiber stiffness. The yield tenacity A (Ffb) is the tenacity at which the α-form is partially transformed into the β-form fibril. The relaxation time τ is the time (or the elongation) at which 63% of yield tenacity is reached. τ decreases with the α- to β-form transformation rate. The fibril breaking energy is the

TABLE VI
Parameters of the Model Explaining Fibril and Matrix Tensile Behavior Including the 95% Confidence Interval of the Parameters

	Fibril parameters			Matrix parameters		Determ. coeff's	
Wool ref.	A	B	D	C	E	Adj. R^2	R^2
1. NEW	0.70 ± 0.04	89.4 ± 36.4	1.20 ± 0.09	1.68 ± 0.69	1.61 ± 0.45	99.88%	99.90%
2. METH1	0.71 ± 0.03	142.9 ± 53.0	1.33 ± 0.09	2.00 ± 0.53	1.50 ± 0.29	99.93%	99.94%
3. ACET1	0.65 ± 0.04	165.0 ± 92.6	1.31 ± 0.13	1.84 ± 1.02	1.58 ± 0.54	99.84%	99.87%
4. DCMA	0.78 ± 0.03	185.6 ± 75.1	1.36 ± 0.10	2.00 ± 0.76	1.58 ± 0.37	99.91%	99.93%

TABLE VII
Viscoelastic Parameters of the Mechanistic Model Explaining the Behavior of Fibers during Tensile Testing at a Deformation Rate of 1%.s^{-1}.

Wool ref.	Fiber Breaking elong. [%]	Fibril contribution				Matrix contribution		
		M (cN/dtex)	Ffb = A (cN/dtex)	τ (s)	Wf (cN/dtex)	Mb (cN/dtex)	Fmb (cN/dtex)	Wm (cN/dtex)
NEW	34.1	62.6	0.70	1.12	0.18	0.75	0.30	0.04
METH	33.4	101.5	0.71	0.70	0.16	0.80	0.39	0.05
ACET	29.7	107.3	0.65	0.61	0.13	0.68	0.27	0.03
DCMA	30.8	144.8	0.78	0.54	0.15	0.83	0.31	0.04

Elongation at break in (%), Initial modulus M (cN/dtex), yield tenacity A (cN/dtex), relaxation time (or elongation) at which 63% of the yield tenacity is reached, breaking work of the fibrils Wf (cN/dtex). Reinforcing modulus at break Mb (cN/dtex), matrix tenacity at break Fm (cN/dtex), and breaking work of the matrix (cN/dtex).

area under the curve up to the breaking point for the fibril component. The reinforcing modulus at break Mb is directly related to matrix and fiber stiffness at the breaking point. Matrix tenacity at the breaking point Fmb is the contribution of the matrix tenacity at that point, and the matrix breaking energy is the contribution of the matrix to breaking work of the fiber. For comparison, fiber elongation at break is included in Table VII.

The internal wool lipid extraction is related to a decrease in the elongation at break of the fibers, an increase in the initial modulus, and a decrease in the relaxation time. The higher the elongation at break, the higher the breaking work of the fibril component ($r = 0.94$ at 10% of significance). The initial modulus and the relaxation time are highly correlated ($r = -0.92$ significant at 10% level). This could confirm the hypothesis that the IWL could act as a plasticizer between the fibrils and matrix, minimizing damage concentrations that could precipitate fibril failure and fracture. Stress concentration increases the conversion rate of fibrils from the α- to the β-form, which takes place at yield tenacity.

The breaking tenacity and the reinforcing modulus at break are highly correlated ($r = 0.97$ at 5% of significance). The reinforcing modulus is directly related to yield tenacity ($r = 0.93$ at 10% of significance), which highlights the role of the fibrils in fiber tenacity.

Regarding the matrix component, a logical relationship between breaking tenacity and breaking can also be noted ($r = 0.96$ at 5% of significance).

It should be pointed out that fiber breaking depends on both the fibril contribution and the stress concentration that could precipitate fibril failure and fracture. The plasticizer effect of IWL favors the distribution of the remote stress locally placed by minimizing damage concentrations and allowing the fiber to continue to function almost normally by absorbing higher energy levels before its catastrophic failure.

CONCLUSIONS

The extraction with acetone and methanol solvents supply good yields of IWL extracts (0.8% and 1.4% o.w.w). Although the extraction with methanol achieves the richest extracts, the chemical modification undergone by the fiber subjected to this treatment should be pointed out. Even though no significant modifications were observed in the mechanical tests performed, the lower whiteness and the higher yellowness indexes plus the high extract of lipids indicate a possible alteration of the fibers, which could affect their further use in the textile process.

On the other hand, acetone-extracted fibers have a lower alkaline solubility, a superior fiber length and barb, and a whiteness index similar to that of nonextracted fibers. A possible explanation for this behavior could be an increase in the protein reticulation of the fibers due to the acetone treatment.

Tensile behavior mainly depends on the fibril component of wool fibers. The lipid extraction may affect the transference of stresses between fibrils and matrix. In this article, we provide evidence that samples submitted to lipid extraction show poorer transference of stresses. In our opinion, this could favor the stress concentration phenomena in fibrils, resulting in an increase in yield tenacity and in the conversion rate between the α- to β-form fibrils, and consequently, in a decrease in the elongation at break of the fibers. Thus, it can be concluded that a prior extraction of the IWL increases yield tenacity and decreases the elongation at break of the fibers, while maintaining the feasibility of extracted wool for textile purposes.

We acknowledge the technical assessment of Mr. J. Sánchez from SAIPEL. Thanks are also due to Mrs. I. Yuste and Mr. G. von Knorring for his technical support.

References

1. Leeder, J. D.; Rippon, J. A. J Soc Dyers and Colourists 1985, 101, 11.

2. Hearle, J. W. S. J Appl Polym Sci Appl Polym Symp 1991, 47, 1.
3. Mercer, E. H. J Soc Cosmet Chem 1965, 16, 507.
4. Rogers, G. E. J Ultrastruct Res 1959, 2, 309.
5. Ward, I.; Hadley, D. M. In An Introduction to the Mechanical Properties of Solid Polymers; John Wiley & Sons: Chichester, 1993.
6. Speakman, J. B. J Text Inst 1927, 18, T431.
7. Bendit, E. G. In Proc. Int. Wool Textile Research Conf., Pretoria, 1980, p. 43, vol. II.
8. Feughelman, M. Text Res J 1963, 33, 1013.
9. Bondia, I.; Sanchez, J.; Manich, A. M.; Martí, M.; Parra, J. L.; Coderch, L. IWTO Barcelona Meeting, Report No. CTF 06, 2002.
10. Manich, A. M.; Ussman, M. H.; Barella, A. Text Res J 1999, 69, 325.
11. Manich, A. M.; Marino, P. N.; de Castellar, M. D.; Saldivia, M.; Saurí, R. M. J Appl Polym Sci 2000, 76, 2026.
12. IWTO-6-86: Air Flow.
13. IWTO-17-85: Almeter AL100.
14. Ussman, M. H.; Manich, A. M.; Gacén, J.; Maillo, J. J Text Inst 1999, 90(Part 1), 526,
15. Manich, A. PhD Thesis. Technical University of Catalonia, Barcelona, 1990.
16. Attenburrow, G. E. J Soc Leather Tech Chem 1993, 77, 107.
17. Draper, N.; Smith, H. In Applied Regression Analysis; J. Wiley and Sons: New York, 1981, p. 91.
18. Coderch, L.; Fonollosa, J.; Martí, M.; Garde, F.; de la Maza, A.; Parra, J. L. J Am Oil Chem Soc 2002, 79, 1215.
19. Coderch, L.; Fonollosa, J.; Martí, M.; Garde, F.; Parra, J. L. Proc. 10th Int. Wool Tex. Res. Conf., Aachen, 2000, Report ST-11.
20. Schwan, A.; Herrling, J.; Zhan, H. Colloid Polym Sci 1986, 264, 171.
21. Leeder, J. D. Wool Sci Rev 1986, 63, 3.
22. Statgraphics Plus for Windows, Manugistics, Inc., 2115 East Jefferson Street, Rockville, MD 20852-4999.